Published in final edited form as:
Mol Cancer Res. 2009 July ; 7(7): 1086–1098. doi:10.1158/1541-7786.MCR-08-0361.

Potentiation of cannabinoid-induced cytotoxicity in Mantle Cell Lymphoma through modulation of ceramide metabolism

Kristin Gustafsson[1)], **Birgitta Sander**[1)], **Jacek Bielawski**[2)], **Yusuf A. Hannun**[2)], and **Jenny Flygare**[1)]

[1)] Department of Laboratory Medicine, Division of Pathology Karolinska Institutet and Karolinska University Hospital Huddinge, F-46, SE-14186 Stockholm, Sweden

[2)] Department of Biochemistry and Molecular Biology Medical University of South Carolina, Charleston, South Carolina 29425, USA

Abstract

Ceramide levels are elevated in Mantle Cell Lymphoma cells following treatment with cannabinoids. Here, we investigated the pathways of ceramide accumulation in the MCL cell line Rec-1 using the stable endocannabinoid analogue *R*(+)-methanandamide (R-MA). We further interfered with the conversion of ceramide into sphingolipids that promote cell growth. Treatment with R-MA led to increased levels of ceramide species C_{16}, C_{18}, C_{24} and $C_{24:1}$ and transcriptional induction of ceramide synthases (CerSs) 3 and 6. The effects were attenuated using SR141716A, which has high affinity to cannabinoid receptor 1 (CB1). The CB1-mediated induction of CerS3 and CerS6 mRNA was confirmed using Win-55,212-2. Simultaneous silencing of CerS3 and CerS6 using siRNA abrogated the R-MA-induced accumulation of C_{16} and C_{24}. Inhibition of either of the enzymes serine palmiotyl transferase, ceramide synthase, and dihydroceramide desaturase within the *de novo* ceramide pathway reversed ceramide accumulation and cell death induced by R-MA treatment. In order to enhance the cytotoxic effect R-MA, sphingosine kinase-1 (SK-1) and glucosylceramide synthase (GCS), enzymes that convert ceramide to the pro-proliferative sphingolipids sphingosine-1-phospate and glucosylceramide, respectively, were inhibited. Suppression of either enzyme using inhibitors or siRNA potentiated the decreased viability, induction of cell death and ceramide accumulation induced by R-MA treatment. Our findings suggest that R-MA induces cell death in MCL via CB1-mediated upregulation of the *de novo* ceramide synthesis pathway. Furthermore, inhibition of SK-1 and GCS potentiated ceramide accumulation and cell death induced by R-MA. This is the first study were the cytotoxic effect of a cannabinoid is enhanced by modulation of ceramide metabolism.

INTRODUCTION

Ceramide accumulation is a widely described event in cancers after various treatments [1]. C_{16}-Ceramide is described as one of the major ceramide sub-species whose levels are elevated during apoptosis induced by various agents [2]. For instance, C_{16} ceramide, generated *de novo*, was accumulated during androgen ablation in the prostate cell line LNCaP [3]. Both C_{16} and C_{24} ceramide accumulated during BcR crosslinking in Ramos cells [4,5]. When ceramide species C_{18} was specifically induced in UM-SCC-22A cells (sqaumous cell carcinoma of hypopharynx) by overexpression of CerS1, cell growth was inhibited [6].

Address correspondence to: Kristin Gustafsson, F-46, Karolinska Sjukhuset, Huddinge SE-14186 Stockholm, Sweden., Fax: 0046-85858-7730, kristin.gustafsson@ki.se.

In previous publications [7–9] we and others observed that induction of ceramide accumulation by cannabinoids leads to apoptosis in MCL, glioma and pancreatic cancer. The signaling leading to cell death was blocked by inhibition of ceramide synthase with Fumonisin B1 (FB1). In MCL, the accumulation of ceramide was mediated through the cannabinoid receptors type 1 (CB1) and type 2 (CB2) which are overexpressed on MCL cells, while control cells lacking the receptors remained unaffected.

There are six species of ceramide synthases (CerSs), and several iso-forms have been described [2]. CerSs 1–6 synthesize ceramides of varying chain length [2]. When CerS3 was overexpressed in HEK-293T cells, an increased production of C_{18} and C_{24} ceramide species was observed [10], while overexpression of CerS6 showed that the enzyme preferably synthesized the long chain ceramide species C_{14} and C_{16} ceramide [11].

CerSs can act through two different pathways, as they are involved in both *de novo* synthesis of (dihydro)ceramide as well as regeneration of ceramide from sphingosine in the salvage/recycling pathway, see Fig 1. Several enzymes are involved in the *de novo* synthesis of ceramide which starts with the precursors L-serine and palmitoyl-CoA. Their conversion into 3-ketosphinganine is catalyzed by Serine Palmitoyl Transferase (SPT) [12]. Further downstream, sphinganine is acylated to dihydroceramide by ceramide synthase (CerS). The dihydroceramide is desaturated by dihydroceramide desaturase (DEGS) to ceramide [13]. On the other hand, in the salvage/recycling pathway, CerSs act on sphingosine that is generated from the breakdown of complex sphingolipids. Since FB1 inhibits CerS, its actions do not distinguish between the activation of the *de novo* pathway vs. the operation of the salvage pathway. Thus, it became important to determine the specific pathway activated by cannabinoids.

Once ceramide is synthesized, it can be rapidly metabolized into sphingomyelin, glucosylceramide or sphingosine, see Figure 1, and the latter two can be further converted to complex glycosphingolipids or sphingosine-1-phosphate (S-1-P), respectively. Metabolism of active ceramide into such species by glucosylceramide synthase (GCS) or sphinogsine kinase-1 (SK-1) is the limiting factor in the cell death response to ceramide-inducing stimuli [1]. It has been shown in multiple cell types [14] that manipulating ceramide metabolism by blocking enzymes leads to a potentiation of cell death. Also, the balance between ceramide and S-1-P is vital to the cell death decision in many cancer types [15] [16]. Safingol, an inhibitor of SK-1, has been shown to synergistically increase the efficacy of the cytotoxic drug fenretinide in neuroblastoma cells [17]. Down regulation of SK-1 by ActD in Molt-4 cells has been shown to decrease viability and induce cell death [18]. Resistant melanoma cells Mel-2a showed increased rate of apoptosis after treatment with siRNA against SK-1 together with Fas antibody CH-11 or C_6-ceramide [19]. Several studies have shown that overexpression of GCS in cancers can generate multidrug resistance caused by subsequent upregulation of the multi drug resistance 1 (MDR1) gene [20,21]. There are multiple publications stating that GCS inhibitors e.g. PDMP, PPMP and PPPP can enhance the effect of chemotherapeutic drugs in resistant cells [22], [23]. Using antisense to downregulate GCS in resistant breast cancer cells, MCF-7 Adr, Gouaze et al [24] showed a decrease in MDR1 expression leading to an increased cell death by vinblastine.

In our previous publications we have induced cell death by treatment of lymphoma cells with different cannabinoids *in vitro* [7,25], and observed a 40% reduction of tumor burden in NOD/SCID mice xenotransplanted with human MCL by treatment with the stable endocannabinoid analogue *R*(+)-methanandamide (R-MA) *in vivo* [7]. These results together with those implicating ceramide in the action of cannabinoids raised the possibility that preventing the transformation of ceramide into other forms of sphingoplipids could enhance the cell death response in MCL. Further, the Nordic lymphoma Network reported that

adding the chemotherapeutic agents doxorubicine and Ara-C, both inducers of ceramide accumulation, to MCL treatment has improved the event free survival for MCL patients. Thus, ceramide accumulation appears to contribute to the reduction of malignant MCL cells *in vivo*.

In this study, we investigated the mechanisms and specificity of the ceramide response to R-MA. We further exploited this understanding in order to determine if modulating ceramide levels could potentiate the cytotoxic response to R-MA. The obtained data show that R-MA treatment leads to increased expression of ceramide synthases, *de novo* synthesis of specific ceramide species and apoptosis in the MCL cell line Rec-1. Modulation of ceramide metabolism using inhibitors or RNA interference potentiates the apoptosis-inducing effect of R-MA.

Experimental procedures

Reagents and drugs

R(+)-methanandamide (R-MA), Win-55,212-2 (Win55), Fumonisin B1, Myriocin, SKI II, DMS and PDMP were purchased from Sigma-Aldrich Sweden AB (Stockholm, Sweden). C_8-Cyclopropenylceramide (C_8CPPC) was obtained from Matreya LLC (PA, USA). ^{3}[H]-palmitate was purchased from Amersham Biosciences (Buckinghamshire, England). SiRNAduplexes against CerS3, CerS6, GCS and SK1 were purchased from Ambion and diluted to 200nM in siRNA dilution buffer (Qiagen, Valencia, CA). AIM-V medium was purchased from Invitrogen Corporation (Carlsbad, CA).

Cell lines

The MCL cell line Rec-1 was a kind gift from Dr. Christian Bastard, Ronan, France. The plasma cell line SK-MM-2 was obtained from Deutsche Sammlung von Microorganismen und Zellkulturen (DSMZ) (Braunschweig, Germany). Cell lines were maintained in RPMI 1640 medium (Invitrogen, Carlsbad, CA) supplemented with 2 mM L-glutamine and 10% fetal calf serum (FCS) and 50 μg/ml gentamicin (Invitrogen) under standard conditions (humidified atmosphere, 95% air, 5% CO_2, 37°C).

Ceramide analyses HPLC-MSMS

After treatment, samples were frozen at −80 °C and transferred to the Lipidomics Core facility at MUSC. There lipids were measured by high performance liquid chromatography tandem mass spectrometry (MS/MS) as described earlier [26].

Phosphate assay

Phospholipids were extracted according to Bligh and Dyer [27]. The samples and phosphate standards made of NaH_2 PO_4 were ashed in ashing buffer (10 N H_2SO_4: 70% $HClO_4$: H_2O) at 160 °C overnight. Thereafter, 900 μl water, 500 μl 0, 9% ammounium molybdate and 200 μl 9% ascorbic acid was added to each sample followed by incubation at 45 °C for 30 minutes. The amount of lipid phosphate was determined by measuring absorption at 590 nm.

Radioactive lipid analysis

Rec-1 cells were resuspended in AIM-V media containing 2μCi [^{3}H]-palmitic acid to a concentration of 2 million cells/ml. After 12 hrs, cells were washed in PBS and treated with 10μM R-MA with or without pre-treatment with inhibitors in fresh AIM-V media.

Cells were harvested and washed in cold PBS three times. Subsequently, cells were dissolved in 50 μl PBS and the suspension was added to 1 ml of MeOH;$CHCl_3$(1:2). To

extract the lipids, 1 ml water was added to the samples that were centrifuged 20 min at 4°C to attain two distinct phases. The lower phase containing the lipids was dried by SpeedVac for 45 minutes. Lipids were resuspended in 50 μl Chloroform/methanol (2:1). The lipid samples were loaded onto a 60 Ångström silica TLC plate (Scleicher&Schnell, Germany) pre-washed in acetone. The TLC plate was run for 45 minutes in a solvent system for ceramide (90 ml Ethylacetate:50 ml Ocanoic Acid:20 ml Acetic Acid), then dried followed by treatment 3 times with [^{3}H]-enhancer spray. The plate was then developed for 48 hrs at −80°C. To quantify [^{3}H]-ceramide, the area of interest was scraped into 3,5 ml scintillation fluid and analyzed by liquid scintillation. [^{3}H]-ceramide was normalized to total [^{3}H]-labeled cells loaded per lane. Treated samples were compared to vehicle treated control.

RNA isolation

Total RNA was prepared using Qiagen RNA purification system as directed by the supplier (Qiagen, Valencia, CA). The samples were treated with Turbo DNase Kit to eliminate genomic DNA (Ambion, Austin, TX).

cDNA synthesis and real-time quantitative RT-PCR

First strand cDNA synthesis was carried out according to the protocol for Omniscript Reverse Transcription (Qiagen, GmbH, Hilden, Germany). One microgram of RNA was used in the reactions for RT-PCR. The Beacon Designer 3 program (Biosoft International, Palo Alto, CA) was employed for design of primers (See Table 1). Primers were synthesized by Integrated DNA Technologies (Leuven, Belgium). The quantification of CerS compared to β-actin was carried out with an iCycler iQ (Bio-Rad Laboratories, Sundbyberg, Sweden). The iCycler iQ reaction detection system software from the same company was used for data analysis. cDNA was amplified using the qPCR Kit Platinum SYBR Green qPCR SuperMix-UGD with FITC (Invitrogen) according to the manufacturer's instructions. The samples were divided into triplicates in a 96-well PCR plate (Abgene, Hamburg, Germany) and run at 95°C for 10 min followed by 40 cycles, each cycle consisting of 15 sec at 95°C and 1 min at 55°C. Threshold (Ct) cycle numbers were obtained from amplification of primers (Table 1). ΔCt values were calculated by subtracting the Ct value of β-actin from the Ct value of primers for the genes of interest. The relative fold increase (RFI) of the genes of interest was calculated as follows. The ΔCt for controls and treated samples was first determined. The ΔCt value was calculated by subtracting the Ct value for housekeeping control from the Ct value for the gene of interest. The RFI of genes of interest was calculated by the equation: $RFI = 2^{-\Delta Ct}$. To use this calculation, the PCR efficiencies of the target and control assays must be similar. This was achieved by adjusting primer concentrations. The criterion for using the ΔCt method was fulfilled because by graphing serial dilutions of input cDNA of a random sample against ΔCt values (genes of interest-β-actin), the slope of the line as $\ll 0.1$ (data not shown).

Cell Death ELISA

Cell Death ELISA (Roche, Mannhein, Germany) is a quantitative sandwich ELISA that detects histone and intra-nucleosomal DNA fragmentation by binding to two different monoclonal antibodies. It allows specific determination of mono- and oligonucleosomes in the cytoplasmatic fraction in cell lysates. The anti-histone-biotin antibody binds to histones H1, H2A, H2B, H3 and H4. The Anti-DNA-POD antibody reacts with double or single stranded DNA in the cytoplasm. In brief, cells were washed and resuspended in AIM-V medium. After treatment (see individual experiments in Results) cells were harvested and lysed with lysis buffer (Roche). The cell lysate was allowed to bind to the enzyme immunoassay plate for two hours together with immunoreagent containing anti-DNA-POD and anti-histone-biotin and incubation buffer. Thereafter, ABTS substrate (Roche,

Mannheim, Germany) was added for 10 min. Adding stop solution terminated the reaction, and the absorption was determined at 405 nm.

Electroporation

The cells were split 2 days before the experiment in order to assure that they are in logarithmic phase during electroporation. On the day of electroporation, 5 million cells were resuspended in 100 μl of Nucleofector solution C (Amaxa Biosystems, Gaithersburg, MD)/ sample. To the cell suspension, 20nM of duplex siRNA was added. The sample was then electroporated using Amaxa Nucleofector Systems, program X-001 (Amaxa Biosystems, Gaithersburg, MD). The electroporated cells were then resuspended in 2,5 ml pre-heated RPMI media supplemented with 10% FBS. Transfection efficiency was evaluated by quantitative PCR.

Cell viability

Viability of cells treated with R-MA and various modulators of ceramide metabolism was determined by using the XTT kit (Roche Diagnostics, Germany) according to manufacturer's instructions. Absorbance was measured at 490 nm and reported as optical density.

Statistical Analysis

Quantitative Cell Death ELISA was evaluated using the Kruskal-Wallis test comparing control and treated cells. P-values are presented in figure legends. The software Statistica (Statsoft AB, Tulsa, OK) was used.

RESULTS

Treatment with Methanandamide induces accumulation of different ceramide species in Mantle Cell Lymphoma

We have previously shown that treatment of MCL cells with cannabinoids leads to an accumulation of ceramide [7]. The effect was mediated by the cannabinoid receptors CB1 and CB2. To further study the time-course of ceramide accumulation, the MCL cell line Rec-1 was treated with 10 μM *R*(+)-methanandamide (R-MA), and total [^{3}H]-ceramide was analysed using tritium labeling and liquid scintillation. After 30 min of treatment, only a slight increase in [^{3}H]-ceramide accumulation was observed compared to the mock-treated control. After four hrs, there was a 30% increase in the accumulation of [^{3}H]-ceramide, which was even more pronounced after 12 or 24 hrs (Fig 2).

The induction of ceramide in MCL is dependent of signaling via the CB1 receptor [7]. To investigate the accumulation of different ceramide species, Rec-1 cells, which express the CB1 receptor, were treated with increasing doses of R-MA. As a control, the cell line SKMM, which has higher endogenous levels of ceramide C_{16} but lacks CB1 expression, was used. The cell lines were treated for 12 hrs with R-MA, and the levels of ceramide species were measured by HPLC/MSMS. A 2–3.5 fold increase of ceramide species C_{16}, C_{18}, C_{24} and $C_{24:1}$ was observed when the MCL cell line Rec-1 was treated with 5 or 10 μM R-MA, while lower doses had no effect (Fig 3a). The levels of ceramide species C_{14}, C_{20}, C_{22}, $C_{22:1}$, C_{26} and $C_{26:1}$ remained unaltered (data not shown). No accumulation of any of the ceramide species was observed after stimulation of the control cell line SKMM with R-MA (Fig 3a). These results show that R-MA induced a subset of ceramide species specifically in MCL. Pre-treatment with SR141716 (SR1) an antagonist with high affinity for CB1, significantly prevented the accumulation of ceramide species C_{16}, C_{18} and C_{24}, while SR144528 (SR2), which binds to CB2, partially inhibited the accumulation of C_{16} and

C_{18} (Fig 3b). These results indicate that R-MA causes accumulation of specific ceramide species mainly via the CB1 receptor.

Methanandamide treatment induces selective up regulation of ceramide synthases 3 and 6 in Rec-1 cells

The relatively late increase in total ceramide levels following treatment with methanandamide raised the possibility that transcriptional upregulation of the CerSs could contribute to the accumulation of ceramide. Therefore, Rec-1 cells and SKMM cells were treated with 10μM R-MA (Fig 4a upper panel) for 12 hrs, and the expression of CerSs was investigated by quantitative real time PCR. In Rec-1, CerS3 and CerS6 showed a 2 and 2.6-fold increase of expression, respectively, after R-MA treatment. In contrast, CerS1 variant 2 showed decreased expression, while the expressions of CerS1 variant 1, CerS2, CerS4 and CerS5 were only marginally altered (Fig 4a upper panel). There was no substantial increase in the expression of CerSs in the control cell line SKMM. These results were confirmed using 10 μM of the synthetic cannabinoid Win-55,212-1 (Win55) (Fig 4a lower panel). When Rec-1 cells were pre-treated with 10nM of SR1, the induction of CerS3 and CerS6 was inhibited to a large extent (Fig 4b). SR2 caused a partial inhibition of the R-MA-induced upregulation of CerS3, while the attenuation of the induction of CerS6 in response to R-MA and of both CerSs in response to Win-55 was not significant (Fig 4b).

To investigate if the upregulation of CerSs following treatment with R-MA gave rise to increased accumulation of ceramides, Rec-1 cells were transfected with siRNA against CerS3 and CerS6. No change in accumulation of ceramide subspecies was observed when either enzyme was silenced. However, when both CerS3 and CerS6 were knocked down simultaneously, the accumulation of ceramide species C_{16} and C_{24} was abrogated (Fig 4c). Thus, CerS3 and CerS6 together appear to contribute to part of the earlier observed synthesis of ceramide species (Fig. 3) in response to treatment with R-MA. Similarly, suppression of both CerS3 and CerS6 caused a reproducible, but non-significant, decrease in the cell death induced by 10 μM R-MA (Fig. 4d).

Inhibition of enzymes in the de novo ceramide pathway leads to decreased ceramide accumulation and decreased cell death in response to R-MA treatment

To delineate the pathway leading to synthesis of ceramide after stimulation with R-MA, inhibitors targeting enzymes in the *de novo* pathway were used. Cells were labeled with radioactive tritium and pretreated with Myriocin, Fumonisin B1 (FB1) or C_8CPPC, inhibitors to SPT, CerSs and DEGS, respectively [28–30] (Fig. 1), prior to treatment with 10μM R-MA. The formation of ceramide was disrupted following pre-treatment with each of these inhibitors (Fig 5a), strongly suggesting that ceramide was synthesized through the *de novo* pathway and not from the salvage pathway. The study was extended by analyzing different ceramide species using HPLC/MS/MS. After treatment with inhibitors and R-MA as described above, accumulation of ceramide species C_{16}, C_{18}, C_{24} and $C_{24:1}$ was abrogated (Fig 5b).

To examine the role of *de novo* ceramide synthesis in the induction of apoptosis, cell death was estimated using Cell Death ELISA and AnnexinV PI staining combined with flow cytometry. Rec-1 cells were pre-incubated with Myriocin, FB1 or C_8CPPC prior to treatment with 10μM R-MA. When *de novo* synthesis was disrupted, apoptosis induced by R-MA was abrogated (Fig 6a, b). Since these inhibitors act at different stages of the *de novo* pathway, the results show that ceramide (or downstream metabolites) and not dihydroceramide or other upstream metabolites in the *de novo* pathway is the primary mediator. This confirms and extends our previous observations were FB1, an inhibitor of CerS, abrogated the induction of cell death.

Suppression of ceramide-metabolizing enzymes using inhibitors or siRNA potentiates to the decreased viability, increased cell death and ceramide accumulation induced by R-MA

It has been shown in earlier studies [31] that increasing ceramide levels by manipulating ceramide metabolism can sensitize cells to cytotoxic treatment. In order to enhance the targeted cell death induced by cannabinoids in MCL [7], we combined the R-MA treatment with inhibition of two ceramide-metabolizing enzymes; SK-1 and GCS. Rec-1 cells were co-treated with 10μM R-MA and the SK-1 inhibitor SKI II or DMS, and after 72 hrs viability was examined by XTT. Co-treatment with SKI II (Fig 7a upper left panel) or DMS (Fig 7a upper right panel) potentiated the effect of R-MA on its own. Co-treatment with the GCS inhibitors C_9DGJ (Fig 7b lower left panel) and PDMP (Fig 7b lower right panel) had a similar effect. To confirm that the effects observed using the inhibitors of ceramide metabolism in MCL cells were specific, SK-1 and GCS were silenced using siRNA. Rec-1 cells were transfected with 20nM siRNA duplexes binding either to either enzyme prior to treatment with 10 μM R-MA. SiRNA against SK-1 or GCS potentiated the decrease in viability induced by R-MA alone (Fig 7c).

To determine the effect of inhibitors to ceramide metabolism in combination with 10 μM R-MA on induction of apoptosis, Cell Death ELISA was performed. C_9DGJ was used in this experiment since it is more specific to GCS than PDMP [32]. SKI II was used since French et al [33] showed that it specifically inhibits the formation of S-1-P. Rec-1 cells were co-treated as above and analyzed after 24 hrs. In accordance with the decrease in viability, there was a potentiation of cell death when SKI II or C_9DGJ was combined with 10μM R-MA (Fig 8a). The potentiation was confirmed using siRNA against SK-1 and GCS (Fig 8b). Taken together, these results demonstrate that inhibition of the transformation of ceramide into S-1-P or glucosylceramide potentiates the viability-suppressing and cell death-inducing effects of R-MA.

To investigate which ceramide species are converted by SK-1 and GCS in Rec-1, siRNA against each enzyme was used in combination with R-MA. Significantly increased levels of ceramide specie C_{16} were detected when SK-1 was inhibited by siRNA against SK-1 prior to treatment with R-MA (Fig 9a left panel), while the levels of C_{18} remained unaffected (Fig 9a right panel). Co-treatment with R-MA and siRNA against GCS induced significantly increased levels of both ceramide C_{16} and C_{18} (Fig 9b). No change in the levels of C_{24} or $C_{24:1}$ was observed (data not shown). Thus, inhibition of SK-1 or GCS is likely to potentiate cell death in Rec-1 via R-MA induced accumulation of C_{16} or C_{16} and C_{18}, respectively.

DISCUSSION

Ceramide is known to function as a second messenger in different cellular processes, e.g. induction of apoptosis and differentiation, and its accumulation can be induced by a variety of stimuli [16]. Cannabinoids have been shown to induce ceramide accumulation in pancreatic cancer-, glioma- and leukemia cell lines [8,9,34] as well as in MCL [7]. The production of ceramide following treatment with cannabinoids can be caused by either hydrolysis of sphingomyelin or *de novo* ceramide synthesis [35,36]. In the current study, we have shown accumulation of ceramide species C_{16}, C_{18}, C_{24} and $C_{24:1}$ in the MCL cell line Rec-1 after long-term stimulation with the stable endocannabinoid analogue R-MA. Ceramides exhibit a tissue-dependent bias for amide-linked fatty acids, characterized by chain length, degree of saturation and degree of hydroxylation. C_{16} ceramide is known to be most abundant in fibroblasts, endothelial cells and immune cells [37,38]. In accordance with the present study using a cell line of B-cell origin, C_{16} and C_{24} ceramide species were accumulated after BcR crosslinking in the B-cell line Ramos [4,5].

It has been shown previously that cannabinoids can induce apoptosis via *de novo* synthesis in C6 glioma cells [36]. In the same study, increased activity of SPT was the rate-limiting step in ceramide synthesis *de novo* [39]. Here, we observed upregulation of messages for ceramide synthases within the same pathway. The six known forms of CerSs are active in two processes, acylating either dihydrosphingosine to form dihydroceramide or sphingosine to form ceramide. After stimulation with R-MA, the Rec-1 cells overexpressed CerS3 and CerS6 two and 2,6 times respectively. CerS6 is a major CerS that is expressed at high levels in a variety of tissues [11], and is associated with synthesis of ceramide species C_{14} and C_{16}. CerS3 is regarded as a minor CerS that has mainly been described in skin and testis [10,40], and has been shown to synthesize the longer ceramide species C_{18}, C_{20} and C_{24} [10,11]. The induction of CerS3 after stimulation with cannabinoids is intriguing, since database searches show that CerS3 expression is rarely present in lymphoma tissue, while CerS6 expression is present in a majority of the lymphomas (Omnibus GEO database).

Silencing of either CerS3 or CerS6 using siRNA had no effect, while simultaneous knockdown abrogated the accumulation of C_{16}, C_{18} and C_{24}. Our results suggest that CerS3 and CerS6 may have redundant functions in the production of ceramide species, and indicate that CerS6 and CerS3 are not restricted to the synthesis of C_{14} and C_{16} or longer ceramide species, respectively. Similarly to the effects on ceramide accumulation, simultaneous suppression of CerS3 and CerS6 had a reproducible, but non-significant inhibitory effect on R-MA-induced cell death. Generally, the induction of ceramide accumulation and cell death following R-MA treatment was greater in untransfected compared to transfected cells, as observed when comparing Fig 3 and 4d or Fig 8a and 8b, respectively. Thus, electroporation itself is likely to affect the background levels of ceramides and DNA fragmentation, rendering the effects of R-MA less pronounced.

The CB1 antagonist SR1 completely inhibited the R-MA-induced accumulation of ceramide species C16, C18 and C24 and the upregulation of CerS3 and CerS6 following treatment with R-MA or Win55. SR2, an antagonist to CB2, partially inhibited the increase in C16, C18 and CerS3, while the inhibitory effects on the accumulation of other ceramide species and on the upregulation of CerS6 were not significant. Given the selectivity of R-MA towards CB1, it may seem surprising that SR2 counteracted the induction of ceramide accumulation and the upregulation of CerSs. These results are in accordance with our earlier studies showing that antagonists to either CB1 or CB2 attenuated cell death induced by R-MA in MCL and other lymphomas expressing both receptors [7,41]. At the doses used, it is possible that R-MA acts as an agonist also to CB2, despite its much higher affinity to CB1. Alternatively, the binding of SR2 to CB2 induces changes downstream of the receptor that affect the signaling via CB1.

We have previously blocked cell death in Rec-1 cells by inhibiting CerSs with FB1 [7]. The same inhibitor has been used to prevent induction of ceramide accumulation by cannabinoids in glioma cells [42]. However, CerSs can act in two pathways; both in regeneration of ceramide from sphingosine and in *de novo* synthesis, see Fig 1. To exclude the involvement of SL degradation, we here added inhibitors to enzymes that are active only in the *de novo* pathway; SPT and DEGS. Dbaibo et al. [43] have shown that inhibition of SPT with myriocin abrogates cell death induced by arsenic trioxide in T-cell leukemia and lymphoma. In the present study, inhibition of either of three different enzymes, SPT, CerS and DEGS, led to an abrogation of ceramide accumulation and suppression of cell death in MCL (Fig 1). This fortifies the role of *de novo* synthesis in the responses to R-MA.

It has previously been suggested that ceramide is the active mediator of apoptosis, while dihydroceramide is merely an inactive precursor to ceramide [14]. In these studies, exogenous ceramide and dihydroceramide have been added to cells or mitochondria [44]

[45]. In contrast, high levels of dihydroceramide were observed in HL-60 leukemia cells prior to cell death, [46] and SMS-KCNR cells were cell cycle arrested when DEGS was inhibited [47]. In our MCL cells, the inhibition of DEGS using C_8-CPPC caused accumulation of dihydroceramide species (data not shown) and inhibited the induction of cell death by R-MA. This supports the theory that dihydroceramide species cannot induce apoptosis when the transformation to ceramide is inhibited.

The above conclusion on the central role of ceramide suggested that the cell death-promoting effects of R-MA could be enhanced by inhibiting the transformation of ceramide into species with opposing effects. Inhibition of both SK-1 and GCS potentiated the effects of R-MA on viability and cell death. French et al [33] have shown that SKI II is a specific inhibitor to S-1-P formation, which also inhibits tumor growth *in vivo*. In view of the significant potentiation of the R-MA-induced effects observed using SKI II *in vitro*, future *in vivo* studies using a combination of R-MA and SKI II in mice xenotransplanted with MCL cells are warranted. To be assured that the effects observed in our experiments were enzyme-specific, GCS and SK1 were silenced using siRNA. In addition to potentiation of the effects induced by R-MA, silencing of SK-1 led to a decrease in cell viability by itself. Taha et al [18] and Sarkar et al [48] have observed that down-regulation of SK-1 by siRNA in MCF-7 cells resulted in a reduction of cell viability. Interference with GCS RNA has also been shown to affect growth of neuroepitelioma [44] and sensitize breast carcinoma cells to cytotoxic drugs [43]. However, the viability of an astrocytoma cell line following treatment with the cannabinoid Δ-9 tetrahydrocannabinol (THC) was not affected by inhibitors or siRNA against GCS [49]. In our cells, knockdown of SK-1 led to significant potentiation of R-MA-induced C_{16} accumulation, whereas the accumulation of both C_{16} and C_{18} was potentiated using siRNA against GCS. Instead, the levels of C_{24} and $C_{24:1}$ remained unaltered. It is possible that these ceramide species are metabolized by other ceramide-converting enzymes, e.g. sphingomyelin synthase or ceramide kinase [1].

In conclusion, we have shown that induction of CerSs regulate *de novo* ceramide synthesis in response to the stable endocannabinoid analogue R-MA in MCL cells. The effect of inhibition of DEGS supports earlier studies showing that ceramide, and not dihydroceramide, is the active mediator of apoptosis. Moreover, inhibition of enzymes that convert ceramide to growth-promoting sphingolipid species potentiated the ceramide accumulation and cell death induced by R-MA in MCL. Cannabinoids have been suggested as a new non-toxic therapeutic option for cancer treatment [50]. This is the first study showing that the cytotoxic effect of a cannabinoid can be enhanced by modulation of ceramide metabolism. The results suggest that interference with ceramide conversion may provide a tool to enhance the targeted cell death-promoting effects of cannabinoids in MCL and other malignant lymphomas overexpressing the CB1 receptor.

Acknowledgments

We thank Dr Alicja Bielawska for her helpful technical advice and comments regarding the manuscript. This study was supported by grants from The Swedish Cancer Society, The Swedish Research Council, The Gunnar Nilsson Cancer Foundation, The Cancer Society in Stockholm, The Magnus Bergvall Foundation, Karolinska Institutet Funds, Stockholm County Council funds, The Fernström funds, The Swedish Society of Medicine, Boehringer-Ingelheim travel fund and NIH (CA87584).

ABBREVIATIONS

MCL	mantle cell lymphoma
***R*(+)-MA**	R(+)-methanandamide

CerS	ceramide synthase
CB1	cannabinoid receptor 1
CB2	cannabinoid receptor type 2
SK-1	sphingosine kinase-1
GCS	glucosyl ceramide synthase
RFI	relative fold increase
SPT	Serine Palmitoyl Transferase
FB1	Fumonisin B1
PDMP	1-phenyl-2-decanoylamino-3-morpholino-propanol
SKI II	Sphingosine Kinase Inhibitor II
DMS	dimethyl sphingosine
MDR1	multi drug resistance gene 1
Myr	Myriocin
C_8CPPC	C_{8-}Cyclopropenylceramide
siRNA	small interfering RNA
RNAi	RNA interference
qPCR	quantitative real-time PCR
MS/MS	tandem mass spectrometry
IS	internal standard
FCS	fetal calf serum
PBS	phosphate buffer saline
SPL	sphingolipid
DEGS	dihydroceramide desaturase

References

1. Ogretmen B, Hannun YA. Biologically active sphingolipids in cancer pathogenesis and treatment. Nature Reviews Cancer. 2004; 4:604–616.
2. Pewzner-Jung Y, Ben-Dor S, Futerman AH. When do Lasses (longevity assurance genes) become CerS (ceramide synthases)?: Insights into the regulation of ceramide synthesis. Journal of Biological Chemistry. 2006; 281:25001–25005. [PubMed: 16793762]
3. Eto M, Bennouna J, Hunter OC, Lotze MT, Amoscato AA. Importance of C16 ceramide accumulation during apoptosis in prostate cancer cells. Int J Urol. 2006; 13:148–156. [PubMed: 16563140]
4. Kroesen BJ, Jacobs S, Pettus BJ, Sietsma H, Kok JW, Hannun YA, de Leij LF. BcR-induced apoptosis involves differential regulation of C16 and C24-ceramide formation and sphingolipid-dependent activation of the proteasome. J Biol Chem. 2003; 278:14723–14731. [PubMed: 12578840]
5. Kroesen BJ, Pettus B, Luberto C, Busman M, Sietsma H, de Leij L, Hannun YA. Induction of apoptosis through B-cell receptor cross-linking occurs via de novo generated C16-ceramide and involves mitochondria. J Biol Chem. 2001; 276:13606–13614. [PubMed: 11278517]
6. Koybasi S, Senkal CE, Sundararaj K, Spassieva S, Bielawski J, Osta W, Day TA, Jiang JC, Jazwinski SM, Hannun YA, et al. Defects in cell growth regulation by C18:0-ceramide and

longevity assurance gene 1 in human head and neck squamous cell carcinomas. Journal of Biological Chemistry. 2004; 279:44311–44319. [PubMed: 15317812]

7. Gustafsson K, Christensson B, Sander B, Flygare J. Cannabinoid receptor-mediated apoptosis induced by R(+)-methanandamide and Win55,212–2 is associated with ceramide accumulation and p38 activation in mantle cell lymphoma. Mol Pharmacol. 2006; 70:1612–1620. [PubMed: 16936228]
8. Carracedo A, Gironella M, Lorente M, Garcia S, Guzman M, Velasco G, Iovanna JL. Cannabinoids induce apoptosis of pancreatic tumor cells via endoplasmic reticulum stress-related genes. Cancer Res. 2006; 66:6748–6755. [PubMed: 16818650]
9. Blazquez C, Carracedo A, Salazar M, Lorente M, Egia A, Gonzalez-Feria L, Haro A, Velasco G, Guzman M. Down-regulation of tissue inhibitor of metalloproteinases-1 in gliomas: a new marker of cannabinoid antitumoral activity? Neuropharmacology. 2008; 54:235–243. [PubMed: 17675107]
10. Mizutani Y, Kihara A, Igarashi Y. LASS3 (longevity assurance homologue 3) is a mainly testis-specific (dihydro)ceramide synthase with relatively broad substrate specificity. Biochem J. 2006; 398:531–538. [PubMed: 16753040]
11. Mizutani Y, Kihara A, Igarashi Y. Mammalian Lass6 and its related family members regulate synthesis of specific ceramides. Biochem J. 2005; 390:263–271. [PubMed: 15823095]
12. Braun PE, Snell EE. Biosynthesis of sphingolipid bases. II. Keto intermediates in synthesis of sphingosine and dihydrosphingosine by cell-free extracts of Hansenula ciferri. J Biol Chem. 1968; 243:3775–3783. [PubMed: 4385606]
13. Geeraert L, Mannaerts GP, van Veldhoven PP. Conversion of dihydroceramide into ceramide: involvement of a desaturase. Biochem J. 1997; 327 (Pt 1):125–132. [PubMed: 9355743]
14. Modrak DE, Gold DV, Goldenberg DM. Sphingolipid targets in cancer therapy. Molecular Cancer Therapeutics. 2006; 5:200–208. [PubMed: 16505092]
15. Alemany R, van Koppen CJ, Danneberg K, Ter Braak M, Meyer Zu Heringdorf D. Regulation and functional roles of sphingosine kinases. Naunyn Schmiedebergs Arch Pharmacol. 2007; 374:413–428. [PubMed: 17242884]
16. Segui B, Andrieu-Abadie N, Jaffrezou JP, Benoist H, Levade T. Sphingolipids as modulators of cancer cell death: potential therapeutic targets. Biochim Biophys Acta. 2006; 1758:2104–2120. [PubMed: 16925980]
17. Maurer BJ, Melton L, Billups C, Cabot MC, Reynolds CP. Synergistic cytotoxicity in solid tumor cell lines between N-(4-hydroxyphenyl)retinamide and modulators of ceramide metabolism. J Natl Cancer Inst. 2000; 92:1897–1909. [PubMed: 11106681]
18. Taha TA, Osta W, Kozhaya L, Bielawski J, Johnson KR, Gillanders WE, Dbaibo GS, Hannun YA, Obeid LM. Down-regulation of sphingosine kinase-1 by DNA damage: dependence on proteases and p53. Journal of Biological Chemistry. 2004; 279:20546–20554. [PubMed: 14988393]
19. Bektas M, Jolly PS, Muller C, Eberle J, Spiegel S, Geilen CC. Sphingosine kinase activity counteracts ceramide-mediated cell death in human melanoma cells: role of Bcl-2 expression. Oncogene. 2005; 24:178–187. [PubMed: 15637591]
20. Liu YY, Han TY, Yu JY, Bitterman A, Le A, Giuliano AE, Cabot MC. Oligonucleotides blocking glucosylceramide synthase expression selectively reverse drug resistance in cancer cells. J Lipid Res. 2004; 45:933–940. [PubMed: 14967819]
21. Sun YL, Zhou GY, Li KN, Gao P, Zhang QH, Zhen JH, Bai YH, Zhang XF. Suppression of glucosylceramide synthase by RNA interference reverses multidrug resistance in human breast cancer cells. Neoplasma. 2006; 53:1–8. [PubMed: 16416005]
22. Olshefski RS, Ladisch S. Glucosylceramide synthase inhibition enhances vincristine-induced cytotoxicity. Int J Cancer. 2001; 93:131–138. [PubMed: 11391632]
23. Dijkhuis AJ, Klappe K, Jacobs S, Kroesen BJ, Kamps W, Sietsma H, Kok JW. PDMP sensitizes neuroblastoma to paclitaxel by inducing aberrant cell cycle progression leading to hyperploidy. Mol Cancer Ther. 2006; 5:593–601. [PubMed: 16546973]
24. Gouaze V, Liu YY, Prickett CS, Yu JY, Giuliano AE, Cabot MC. Glucosylceramide synthase blockade down-regulates P-glycoprotein and resensitizes multidrug-resistant breast cancer cells to anticancer drugs. Cancer Res. 2005; 65:3861–3867. [PubMed: 15867385]

25. Flygare J, Gustafsson K, Kimby E, Christensson B, Sander B. Cannabinoid receptor ligands mediate growth inhibition and cell death in mantle cell lymphoma. FEBS Lett. 2005; 579:6885–6889. [PubMed: 16337199]
26. Bielawski J, Szulc ZM, Hannun YA, Bielawska A. Simultaneous quantitative analysis of bioactive sphingolipids by high-performance liquid chromatography-tandem mass spectrometry. Methods. 2006; 39:82–91. [PubMed: 16828308]
27. Bligh EG, Dyer WJ. A rapid method of total lipid extraction and purification. Can J Biochem Physiol. 1959; 37:911–917. [PubMed: 13671378]
28. Miyake Y, Kozutsumi Y, Nakamura S, Fujita T, Kawasaki T. Serine palmitoyltransferase is the primary target of a sphingosine-like immunosuppressant, ISP-1/myriocin. Biochem Biophys Res Commun. 1995; 211:396–403. [PubMed: 7794249]
29. Triola G, Fabrias G, Casas J, Llebaria A. Synthesis of cyclopropene analogues of ceramide and their effect on dihydroceramide desaturase. J Org Chem. 2003; 68:9924–9932. [PubMed: 14682684]
30. Soriano JM, Gonzalez L, Catala AI. Mechanism of action of sphingolipids and their metabolites in the toxicity of fumonisin B1. Prog Lipid Res. 2005; 44:345–356. [PubMed: 16266752]
31. Radin NS. Killing cancer cells by poly-drug elevation of ceramide levels: a hypothesis whose time has come? Eur J Biochem. 2001; 268:193–204. [PubMed: 11168352]
32. Norris-Cervetto E, Callaghan R, Platt FM, Dwek RA, Butters TD. Inhibition of glucosylceramide synthase does not reverse drug resistance in cancer cells. Journal of Biological Chemistry. 2004; 279:40412–40418. [PubMed: 15263008]
33. French KJ, Upson JJ, Keller SN, Zhuang Y, Yun JK, Smith CD. Antitumor activity of sphingosine kinase inhibitors. J Pharmacol Exp Ther. 2006; 318:596–603. [PubMed: 16632640]
34. Herrera B, Carracedo A, Diez-Zaera M, Gomez del Pulgar T, Guzman M, Velasco G. The CB2 cannabinoid receptor signals apoptosis via ceramide-dependent activation of the mitochondrial intrinsic pathway. Exp Cell Res. 2006; 312:2121–2131. [PubMed: 16624285]
35. Galve-Roperh I, Sanchez C, Cortes ML, del Pulgar TG, Izquierdo M, Guzman M. Anti-tumoral action of cannabinoids: involvement of sustained ceramide accumulation and extracellular signal-regulated kinase activation. Nat Med. 2000; 6:313–319. [PubMed: 10700234]
36. Gomez del Pulgar T, Velasco G, Sanchez C, Haro A, Guzman M. De novo-synthesized ceramide is involved in cannabinoid-induced apoptosis. Biochem J. 2002; 363:183–188. [PubMed: 11903061]
37. Pettus BJ, Kroesen BJ, Szulc ZM, Bielawska A, Bielawski J, Hannun YA, Busman M. Quantitative measurement of different ceramide species from crude cellular extracts by normal-phase high-performance liquid chromatography coupled to atmospheric pressure ionization mass spectrometry. Rapid Communications in Mass Spectrometry. 2004; 18:577–583. [PubMed: 14978803]
38. Pettus BJ, Baes M, Busman M, Hannun YA, Van Veldhoven PP. Mass spectrometric analysis of ceramide perturbations in brain and fibroblasts of mice and human patients with peroxisomal disorders. Rapid Commun Mass Spectrom. 2004; 18:1569–1574. [PubMed: 15282781]
39. Hanada K. Serine palmitoyltransferase, a key enzyme of sphingolipid metabolism. Biochim Biophys Acta. 2003; 1632:16–30. [PubMed: 12782147]
40. Rabionet M, van der Spoel AC, Chuang CC, von Tumpling-Radosta B, Litjens M, Bouwmeester D, Hellbusch CC, Korner C, Wiegandt H, Gorgas K, et al. Male Germ Cells Require Polyenoic Sphingolipids with Complex Glycosylation for Completion of Meiosis: A LINK TO CERAMIDE SYNTHASE-3. J Biol Chem. 2008; 283:13357–13369. [PubMed: 18308723]
41. Gustafsson K, Wang X, Severa D, Eriksson M, Kimby E, Merup M, Christensson B, Flygare J, Sander B. Expression of cannabinoid receptors type 1 and type 2 in non-Hodgkin lymphoma: growth inhibition by receptor activation. Int J Cancer. 2008; 123:1025–1033. [PubMed: 18546271]
42. Blazquez C, Salazar M, Carracedo A, Lorente M, Egia A, Gonzalez-Feria L, Haro A, Velasco G, Guzman M. Cannabinoids inhibit glioma cell invasion by down-regulating matrix metalloproteinase-2 expression. Cancer Res. 2008; 68:1945–1952. [PubMed: 18339876]
43. Dbaibo GS, Kfoury Y, Darwiche N, Panjarian S, Kozhaya L, Nasr R, Abdallah M, Hermine O, El-Sabban M, de The H, Bazarbachi A. Arsenic trioxide induces accumulation of cytotoxic levels of ceramide in acute promyelocytic leukemia and adult T-cell leukemia/lymphoma cells through de

novo ceramide synthesis and inhibition of glucosylceramide synthase activity. Haematologica. 2007; 92:753–762. [PubMed: 17550847]

44. Bielawska A, Crane HM, Liotta D, Obeid LM, Hannun YA. Selectivity of ceramide-mediated biology. Lack of activity of erythro-dihydroceramide. J Biol Chem. 1993; 268:26226–26232. [PubMed: 8253743]
45. Stiban J, Fistere D, Colombini M. Dihydroceramide hinders ceramide channel formation: Implications on apoptosis. Apoptosis. 2006; 11:773–780. [PubMed: 16532372]
46. Tserng KY, Griffin RL. Ceramide metabolite, not intact ceramide molecule, may be responsible for cellular toxicity. Biochem J. 2004; 380:715–722. [PubMed: 14998372]
47. Kraveka JM, Li L, Szulc ZM, Bielawski J, Ogretmen B, Hannun YA, Obeid LM, Bielawska A. Involvement of dihydroceramide desaturase in cell cycle progression in human neuroblastoma cells. J Biol Chem. 2007; 282:16718–16728. [PubMed: 17283068]
48. Sarkar S, Maceyka M, Hait NC, Paugh SW, Sankala H, Milstien S, Spiegel S. Sphingosine kinase 1 is required for migration, proliferation and survival of MCF-7 human breast cancer cells. FEBS Lett. 2005; 579:5313–5317. [PubMed: 16194537]
49. Carracedo A, Lorente M, Egia A, Blazquez C, Garcia S, Giroux V, Malicet C, Villuendas R, Gironella M, Gonzalez-Feria L, et al. The stress-regulated protein p8 mediates cannabinoid-induced apoptosis of tumor cells. Cancer Cell. 2006; 9:301–312. [PubMed: 16616335]
50. Sarfaraz S, Adhami VM, Syed DN, Afaq F, Mukhtar H. Cannabinoids for cancer treatment: progress and promise. Cancer Res. 2008; 68:339–342. [PubMed: 18199524]

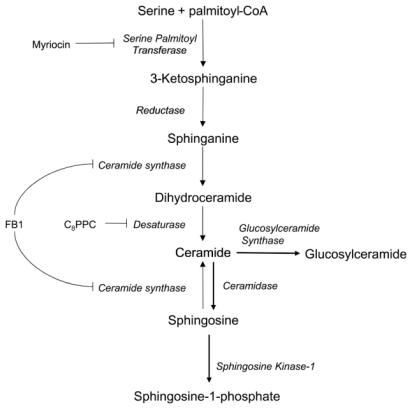

Fig 1. Ceramide metabolism

The enzyme ceramide synthase can synthesize ceramide from sphingosine in addition to catalyzing the conversion of sphinganine to dihydroceramide within the *de novo* ceramide synthesis pathway. Ceramide can be converted to gluosylceramide by glucosylceramide synthase or by sphingosine kinase-1 to sphingosine-1-phosphate.

Abbreviations: FB1- fumonisin B1, C_8CPPC - C_8-cyclopropenylceramide

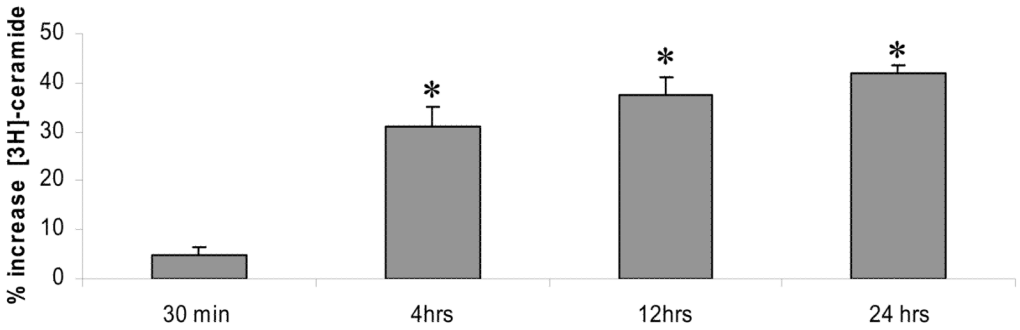

Fig 2. Time-course of the accumulation of total ceramide in response to R-MA

The MCL cell line Rec-1 was labeled with [^{3}H]-palmitic acid followed by treatment with 10μM R-MA for 30 min, 4 hrs, 12 and 24 hrs. Tritiated ceramide was evaluated by liquid scintillation spectroscopy as detailed in Materials and Methods. [^{3}H]-ceramide was normalized against the total number of [^{3}H]-labeled cells loaded per sample. One of three individually performed experiments is shown. *: $p<0.05$ when R-MA treated cells were compared with control cells at the same time-point, Kruskal-Wallis analysis.

Figure 3a

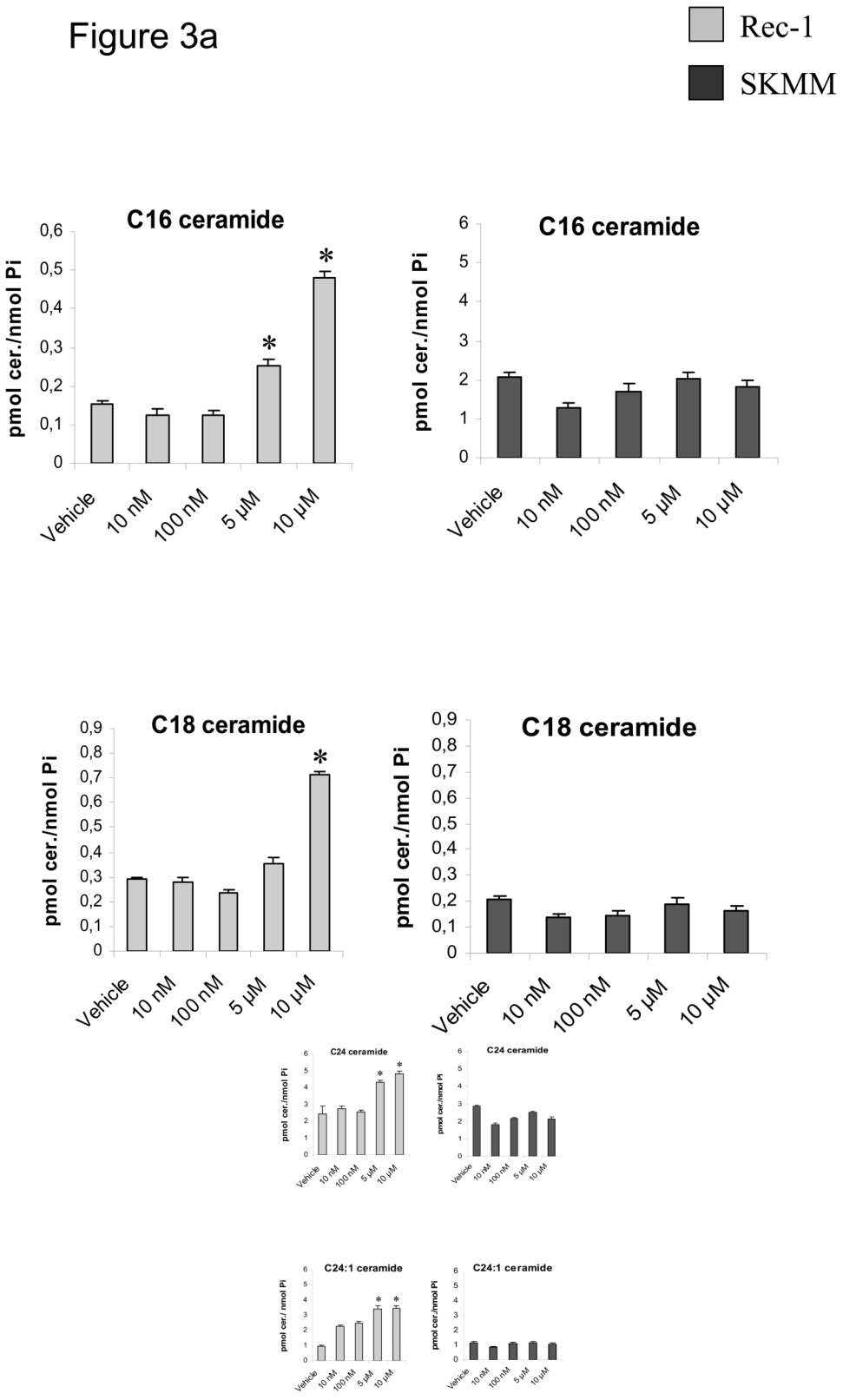

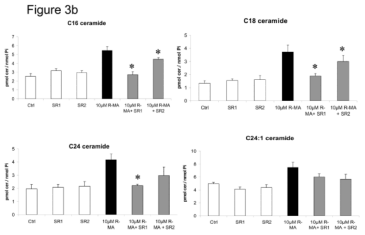

Fig 3. Accumulation of ceramide species C_{16}, C_{18}, C_{24} and $C_{24:1}$ in response to treatment with R_MA

After treatment (see below) cells were prepared for measurement of ceramide using high performance liquid chromatography tandem mass spectrometry as described in Materials and Methods. The masses of the ceramide subspecies C_{16}, C_{18}, C_{24} and $C_{24:1}$ were normalized to lipid phosphate. One of two individually performed experiments is shown. *: $p<0.05$ when R-MA treated cells with and without antagonists were compared using Kruskal-Wallis analysis.

a) The MCL cell line Rec-1 (light grey) and the control cell line SKMM (dark grey) were treated with 10nM, 100nM, 5μM or 10μM of the cannabinoid R-MA for 12 hrs. Due to higher basal levels of C_{16} in SKMM compared to Rec-1 the scales are 10-fold different. **b)** The cell line Rec-1 was pre-treated for 30 min with 10 nM of SR1 or SR2, antagonists to CB1 and CB2, respectively, prior to treatment with 10μM R-MA for 12 hrs.

Figure 4a

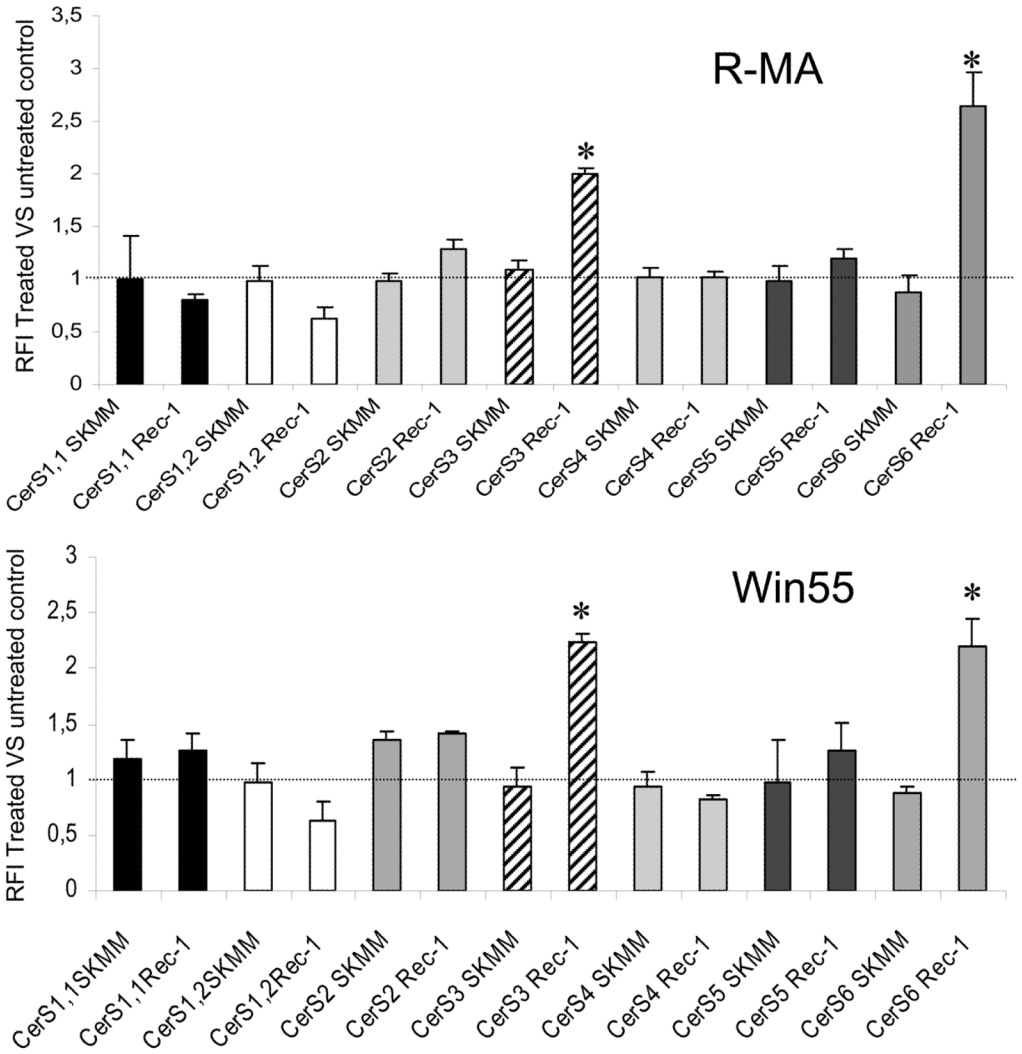

Figure 4b

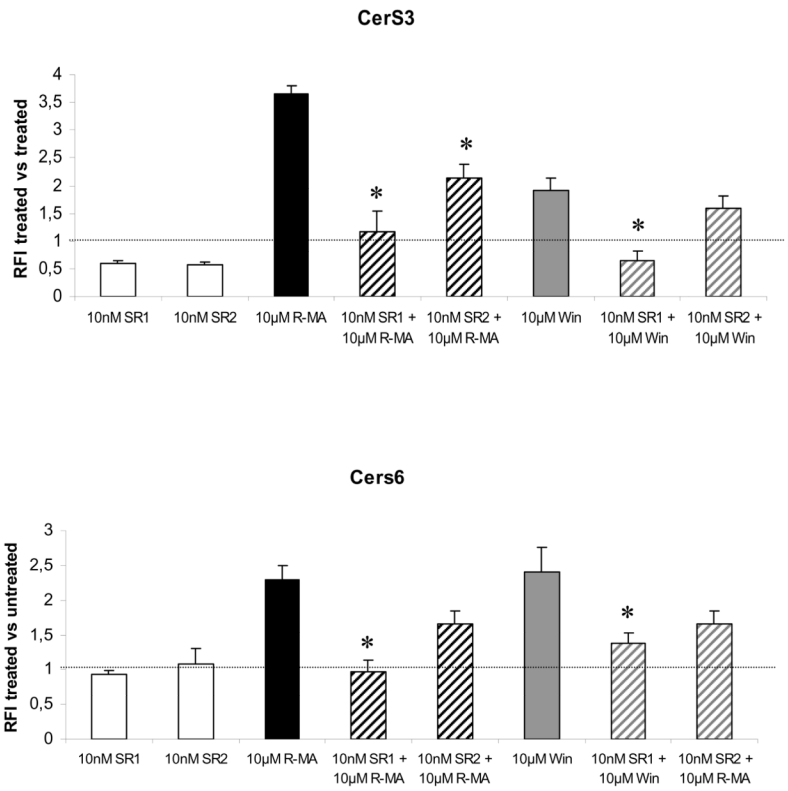

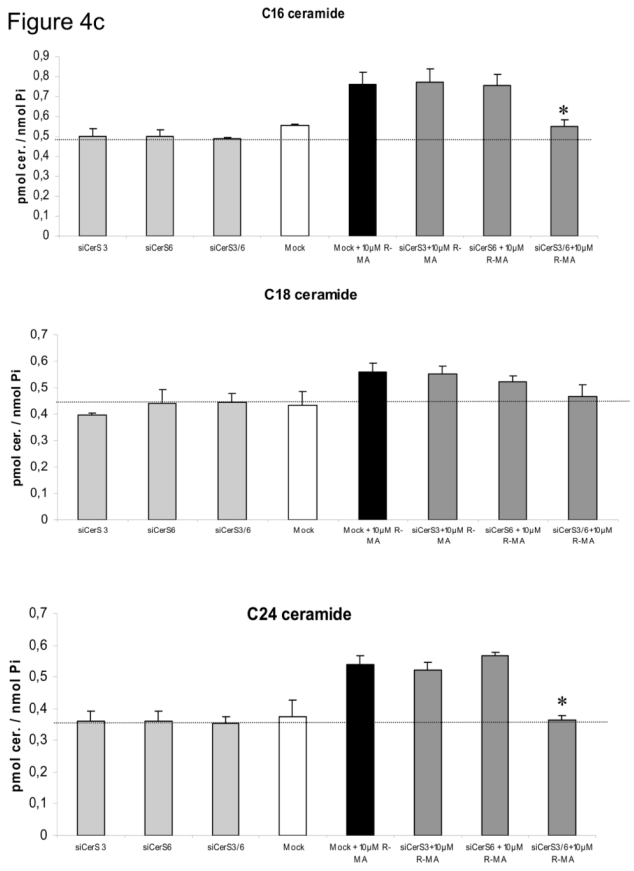

Fig 4. Expression of ceramide synthases after cannabinoid treatment

a) The MCL cell line Rec-1 and the control cell line SKMM were treated for 12 hrs with 10μM R-MA (upper panel) or Win55 (lower panel), or b) Rec-1 cells were pre-treated with 10nM of SR1 or SR2, antagonists to CB1 and CB2, respectively, prior to treatment with 10μM R-MA or Win55 for 12 hrs. After treatment, ceramide synthases (CerS) were detected by quantitative PCR. Values represent relative fold increase (RFI) in the expression of CerS in treated samples compared to control samples. All samples were normalized to the reference gene β-actin. *: $p<0.05$ when R-MA treated cells with and without antagonists were compared using Kruskal-Wallis analysis. c) Rec-1 cells were transfected with siRNA against CerS3 and CerS6. After 24 hrs 10μM R-MA was added for 12 hrs. Measurement of ceramide using high performance liquid chromatography tandem mass spectrometry was performed as described in Materials and Methods. The masses of the ceramide subspecies C_{16}, C_{18}, C_{24} and $C_{24:1}$ were normalized to lipid phosphate. *: $p<0.05$ when R-MA treated cells with and without antagonists were compared using Kruskal-Wallis analysis. d) Rec-1 cells were transfected with siRNA against CerS3 and/or CerS6 and treated with 10 μM R-MA for 12 hrs 24 hrs after transfection. Thereafter, the cell death ELISA was performed. Fluorescence units are shown on the y-axis. One of two individually performed experiments is shown.

Figure 5a

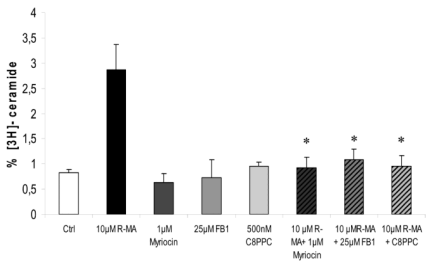

Figure 5b

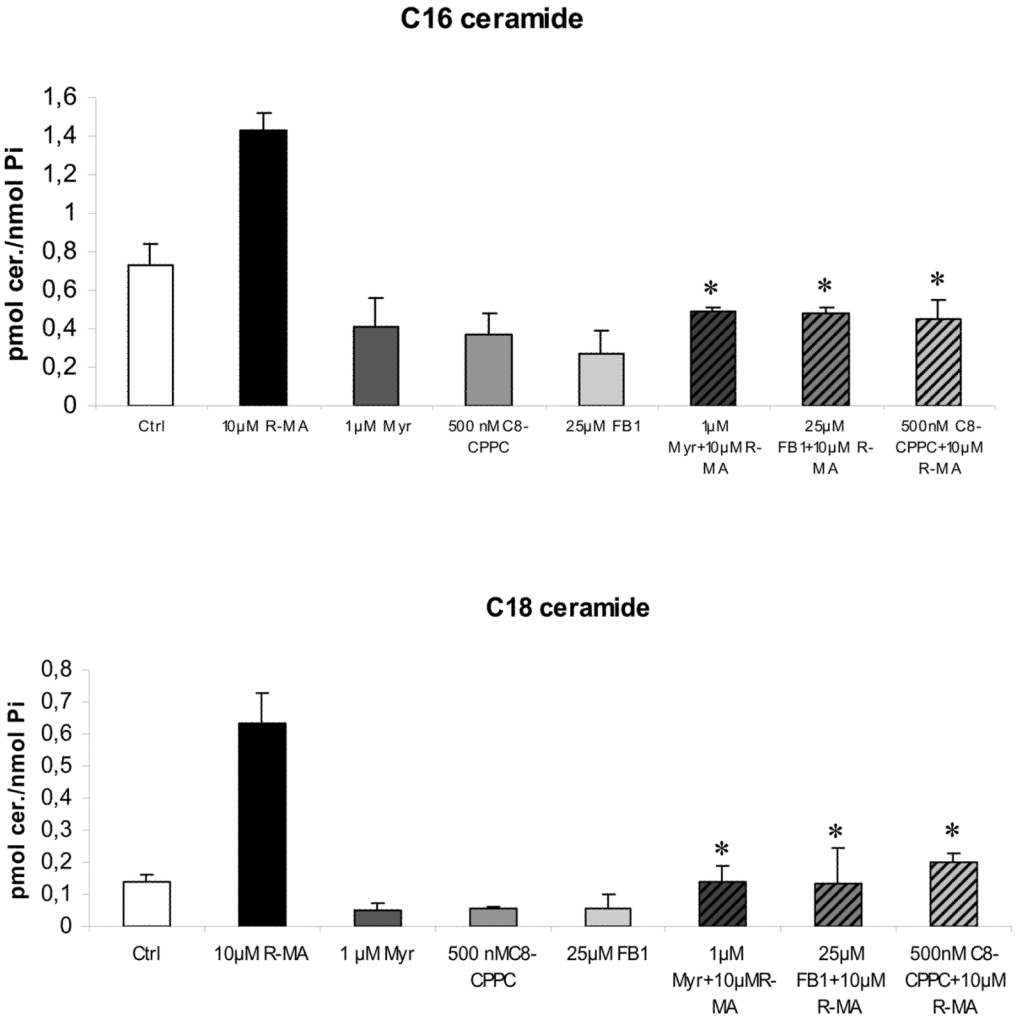

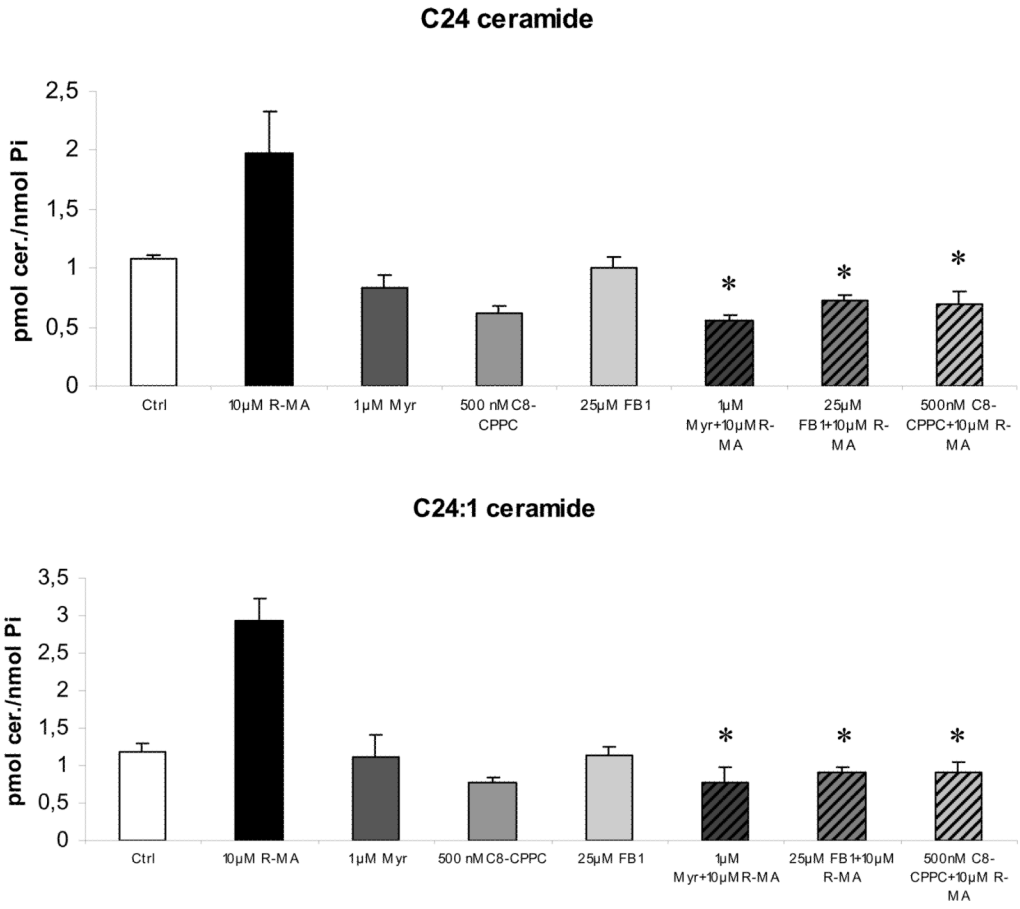

Fig 5. Inhibition of enzymes in the *de novo* synthesis pathway prior to treatment with R-MA leads to disrupted ceramide synthesis

Rec-1 cells were pre-treated for 1 hr with 1μM Myriocin, 25 μM FB1 or 6 hrs with 500 nM C_8-CPPC prior to treatment with 10 μM R-MA for 12 hrs. a) Prior to treatment, the cells were labeled with [^{3}H]-palmitic acid. After treatment [^{3}H]-ceramide was evaluated by liquid scintillation spectroscopy as detailed in Materials and Methods. [^{3}H]-ceramide was normalized against the total number of [^{3}H]-labeled cells loaded per sample. One of two individually performed experiments is shown. *: $p<0.05$ when agonist treated cells with and without inhibitors were compared using Kruskal-Wallis analysis. b) Cells were prepared for measurement of ceramide using high performance liquid chromatography tandem mass spectrometry as described in Materials and Methods. The masses of the ceramide subspecies C_{16}, C_{18}, C_{24} and $C_{24:1}$ were normalized to lipid phosphate. *: $p<0.05$ when agonist treated cells with and without inhibitors were compared using Kruskal-Wallis analysis.

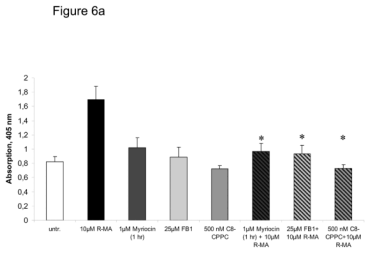

Figure 6b

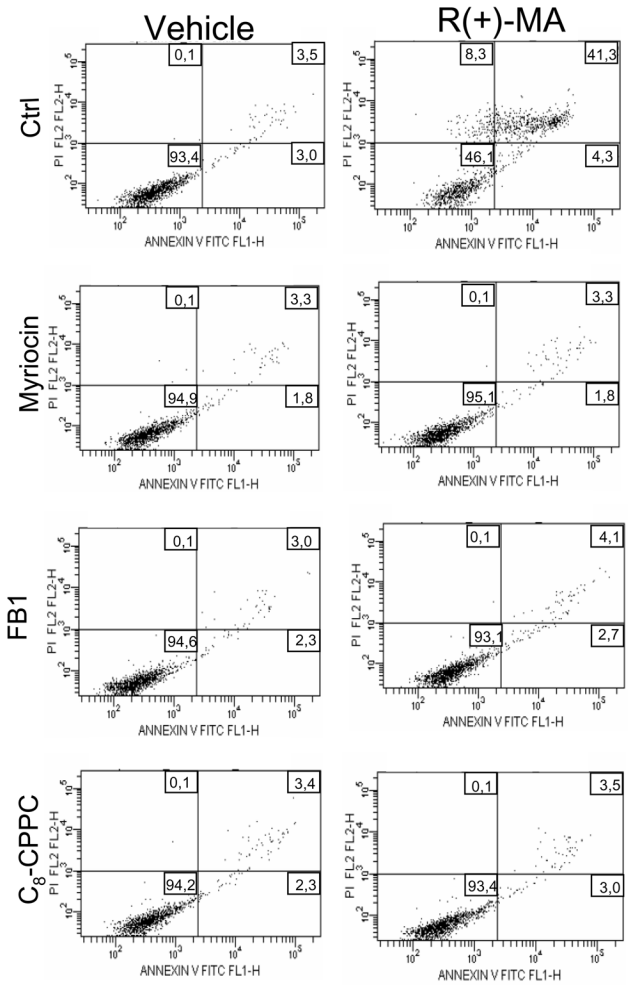

Fig 6. Inhibition of enzymes in the *de novo* ceramide synthesis pathway prior to treatment with R-MA leads to disrupted cell death

The Rec-1 cells were pre-treated for 1 hr with 1μM Myriocin, 25 μM FB1 for 1 hr or 6 hrs with 500 nM C_8-CPPC for 6 hrs followed by treatment with 10μM R-MA for 12 hrs. a) The cell death ELISA was performed, and fluorescence units are shown on the y-axis. One of two individually performed experiments is shown. *: $p<0.05$ when agonist treated cells with and without inhibitors were compared using Kruskal-Wallis analysis. b) Flow cytometry analysis of AnnexinV FITC and PI was performed. Top and bottom right quadrants show late apoptotic/necrotic and early apoptotic cells, respectively. Representative results from three individual experiments are shown.

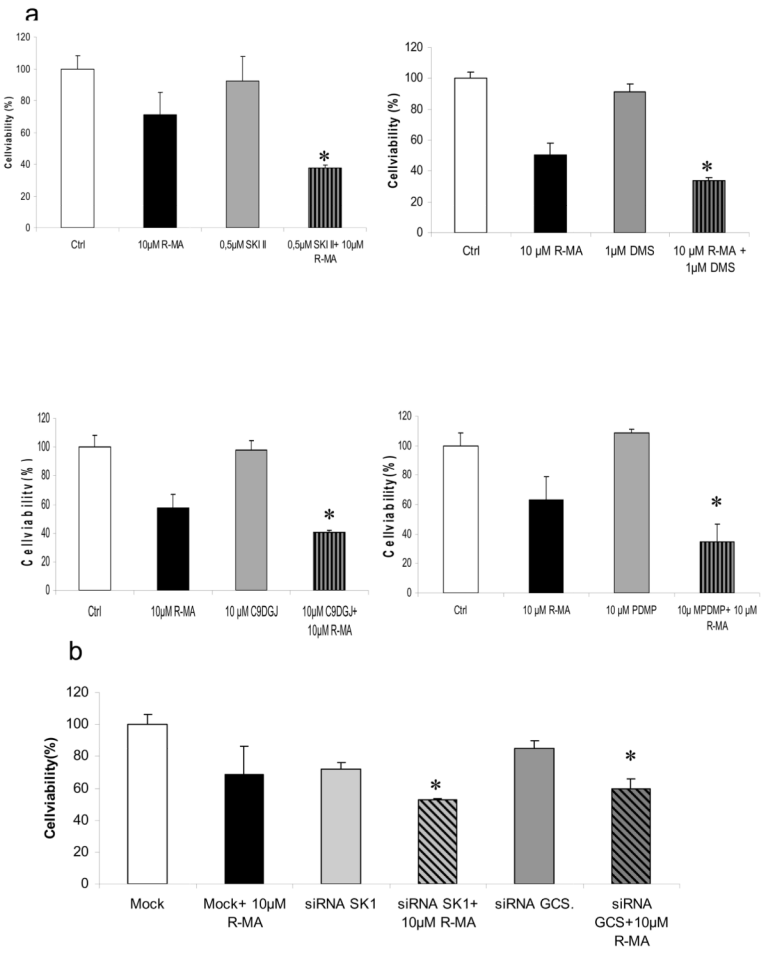

Fig 7. Inhibition of ceramide metabolism potentiates reduction of viability induced by R-MA

Following treatment (see below) viability of treated cells is expressed as percent of vehicle-treated control. One of three individually performed experiments is shown. *: $p<0.05$ when agonist treated cells with and without inhibitors were compared using Kruskal-Wallis analysis. a) Rec-1 cells were treated with 10µM R-MA in combination with 500nM SKI II, 1µM DMS (SK-1 inhibitors), 10 µM C_9DGJ or 10µM PDMP (GCS-inhibitors) for 12 hrs. The XTT assay was performed 72 hrs after treatment. b) Rec-1 cells transfected with siRNA against SK-1 or GCS were treated with 10 µM R-MA for 12 hrs 24 hrs after transfection. The cells were cultured for 48 hrs before XTT assay was performed.

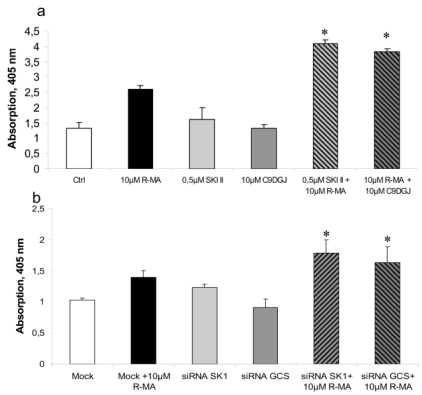

Fig 8. Inhibition of ceramide metabolism potentiates cell death induced by R-MA

After treatment (see below) the cell death ELISA was performed, and fluorescence units are shown on the y-axis. One of two individually performed experiments is shown. *: $p<0.05$ when agonist treated cells with and without inhibitors were compared using Kruskal-Wallis analysis. Rec-1 cells were a) treated with 10μM R-MA in combination with 500nM SKI II (SK-1 inhibitor) or 10μM C_9DGJ (GCS-inhibitor) for 12 hrs or b) transfected with siRNA against SK-1 or GCS and treated with 10 μM R-MA for 12 hrs 24 hrs after transfection.

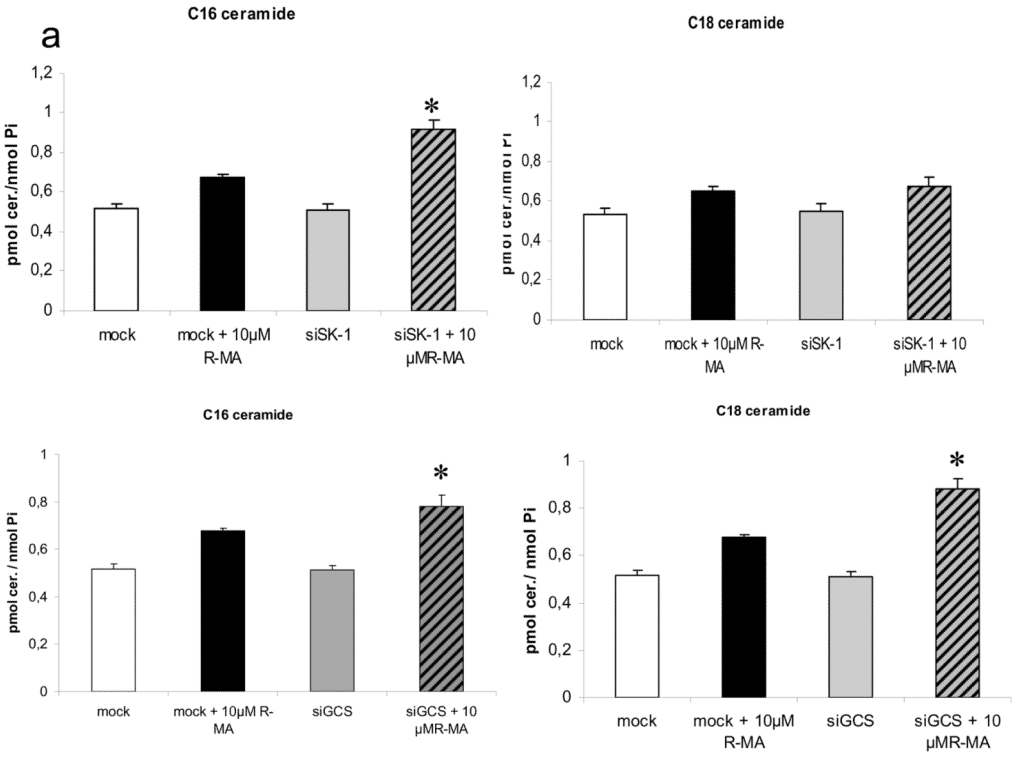

Fig. 9. Effects of inhibition of ceramide metabolism in combination with cannabinoid treatment on accumulation of C_{16} and C_{18}

Rec-1 cells transfected with siRNA against a) SK-1 or b) GCS were treated with 10 μM R-MA for 12 hrs 24 hrs after transfection. After treatment (see below) cells were prepared for measurement of ceramide using high performance liquid chromatography tandem mass spectrometry as described in Materials and Methods. The masses of the ceramide subspecies C_{16} and C_{18} were normalized to lipid phosphate. One of two individually performed experiments is shown. *: $p<0.05$ when agonist treated cells with and without inhibitors were compared using Kruskal-Wallis analysis.

Table 1

Primer sequences used for qPCR

Target	Forward primer 5′-3′	Reverse primer 5′-3′
CerS1, Var1	ACGCTACGCTATACATGGACAC	AGGAGGAGACGATGAGGATGAG
CerS1, Var2	ACGCTACGCTATACATGGACAC	GGAGACGATGAGGATGAGAGTG
CerS2	CCGATTACCTGCTGGAGTCAG	GGCGAAGACGATGAAGATGTTG
CerS3	ACATTCCACAAGGCAACCATTG	CTCTTGATTCCGCCGACTCC
CerS4	CTTCGTGGCGGTCATCCTG	TGTAACAGCAGCACCAGAGAG
CerS5	GCCATCGGAATCAGGAC	GCCAGCACTGTCGGATGT
CerS6	GGGATCTTAGCCTGGTTCTGG	GCCTCCTCCGTGTTCTTCAG
β-actin	ACCTGACTGACTACCTCATGAAGA	GCGACGTAGCACAGCTTCTC

Abbreviations: CerS 1 Var1; Ceramide Synthase 1 isoform 1, CerS 1 Var2; Ceramide Synthase 1 isoform 2, CerS2; Ceramide Synthase 2 CerS3; Ceramide Synthase 3, CerS4; Ceramide Synthase 4 CerS5; Ceramide Synthase 5, CerS6; Ceramide Synthase 6, q PCR; quantitative real-time polymerase chain reaction